

# Large dust fractions can prevent the propagation of soundwaves

Timothée David–Cléris<sup>1\*</sup>, Guillaume Laibe<sup>1,2†</sup>

<sup>1</sup>Univ Lyon, Univ Lyon1, Ens de Lyon, CNRS, Centre de Recherche Astrophysique de Lyon UMR5574, F-69230, Saint-Genis-Laval, France.

<sup>2</sup>Institut Universitaire de France

## ABSTRACT

Dust plays a central role in several astrophysical processes. Hence the need of dust/gas numerical solutions, and analytical problems to benchmark them. In the seminal dustywave problem, we discover a regime where sound waves can not propagate through the mixture above a large critical dust fraction. We characterise this regime analytically, making it of use for testing accuracy of numerical solvers at large dust fractions.

**Key words:** (ISM:) dust, extinction — methods: analytical — protoplanetary discs

## 1 INTRODUCTION

Quantitative study of dust is of prime importance in astrophysics. Numerical simulations are used for determining the 3D evolution of dust/gas systems. Providing accurate tests to benchmark these numerical codes is therefore critical to ensure reliability of the results. Astrophysical dust is usually modelled by a pressureless continuum that exchanges momentum with the gas through a drag force (Saffman 1962; Baines et al. 1965; Clair et al. 1970; Marble 1970). Several analytical problems involving advection, waves, shocks, settling or dust/gas instabilities have been used to benchmark dust-/gas codes (e.g. Benítez-Llambay et al. 2019; Stoyanovskaya et al. 2020 and references therein for recent discussions).

The DUSTYWAVE problem consists of the propagation in 1D of a sound wave in such a mixture (Ahuja 1973; Gumerov et al. 1988; Laibe & Price 2011, 2016 – see Sect. 2). DUSTYWAVE is one of the most widely used benchmark, since it associates dust-/gas drag and gas compressibility, both in Lagrangian (e.g. Laibe & Price 2012, 2014a; Lorén-Aguilar & Bate 2014; Booth et al. 2015; Price & Laibe 2015; Stoyanovskaya et al. 2018; Mentiplay et al. 2020) or in Eulerian methods (e.g. Porth et al. 2014; Yang & Johansen 2016; Hubber et al. 2018; McKinnon et al. 2018; Riols & Lesur 2018; Lebreuilly et al. 2019; Moseley et al. 2019). In attempting to benchmark a numerical code against this test, we figured out the existence of a regime at large dust-to-gas ratios where waves cannot propagate. After having recalled briefly the main properties the DUSTYWAVE problem in Sect. 2, we show the existence of this regime, derive analytic values for the corresponding boundaries, provide physical explanations and numerical tests in Sect. 3.

## 2 DISPERSION RELATION

The equations of evolution for a 1D astrophysical dusty mixture are

$$\partial_t \rho_g + v_g \partial_x \rho_g = -\rho_g \partial_x v_g, \quad (1)$$

$$\partial_t \rho_d + v_d \partial_x \rho_d = -\rho_d \partial_x v_d, \quad (2)$$

$$\partial_t v_g + v_g \partial_x v_g = +\frac{K}{\rho_g} (v_d - v_g) - \frac{\partial_x P}{\rho_g}, \quad (3)$$

$$\partial_t v_d + v_d \partial_x v_d = -\frac{K}{\rho_d} (v_d - v_g), \quad (4)$$

where g and d stand for gas and dust respectively (e.g. Garaud et al. 2004) and  $K$  denotes the drag coefficient. Assuming isothermal gas  $P = c_s^2 \rho_g$ , we expand linearly Eqs. 1–4 under the generic form  $a = a_0 + \delta a$ , with  $v_{d0} = v_{g0} = 0$ . One obtains

$$\partial_t \delta \rho_g = -\rho_{g,0} \partial_x \delta v_g, \quad (5)$$

$$\partial_t \delta \rho_d = -\rho_{d,0} \partial_x \delta v_d, \quad (6)$$

$$\partial_t \delta v_g = +\frac{K}{\rho_{g,0}} (\delta v_d - \delta v_g) - c_s^2 \frac{\partial_x \delta \rho_g}{\rho_{g,0}}, \quad (7)$$

$$\partial_t \delta v_d = -\frac{K}{\rho_{d,0}} (\delta v_d - \delta v_g). \quad (8)$$

We decompose the perturbation on Fourier space under the form  $\delta a = \tilde{a} e^{i(kx - \omega t)}$  for each perturbed field, giving the condition

$$\begin{vmatrix} -i\omega & 0 & \frac{ic_s k \rho_{g,0}}{\rho_{g,0} + \rho_{d,0}} & 0 \\ 0 & -i\omega & 0 & \frac{ic_s k \rho_{d,0}}{\rho_{g,0} + \rho_{d,0}} \\ \frac{ic_s k (\rho_{g,0} + \rho_{d,0})}{\rho_{g,0}} & 0 & -i\omega + \frac{1}{t_g} & -\frac{1}{t_g} \\ 0 & 0 & -\frac{1}{t_d} & -i\omega + \frac{1}{t_d} \end{vmatrix} = 0. \quad (9)$$

We obtain the following dispersion relation

$$\omega^4 + \frac{i}{t_s} \omega^3 - c_s^2 k^2 \omega^2 - \frac{i}{t_s} c_s^2 k^2 (1 - \epsilon) \omega = 0, \quad (10)$$

where the barycentric stopping time is  $t_s \equiv \frac{\rho_{g,0} \rho_{d,0}}{K(\rho_{g,0} + \rho_{d,0})}$  and  $\epsilon \equiv \frac{\rho_{d,0}}{\rho_{g,0} + \rho_{d,0}}$  is the total dust fraction. Rescaling time and space

\* timothee.david-cleris@ens-lyon.fr

† guillaume.laibe@ens-lyon.fr

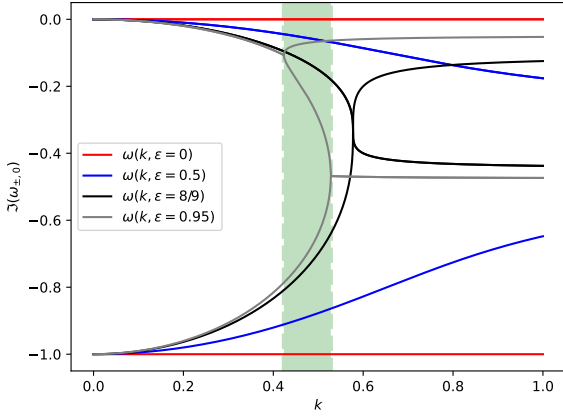


**Figure 1.** Imaginary parts of the roots  $\omega_{\pm}$  and  $\omega_0$  for different values of the dust fraction  $\epsilon$  revealing a bifurcation at  $\epsilon \geq \epsilon_c = 8/9$ .

by  $t_s$  and  $c_s t_s$  respectively gives in the dimensionless form

$$\omega^4 + i\omega^3 - k^2\omega^2 - ik^2(1 - \epsilon)\omega = 0, \quad (11)$$

where we preserved the notations  $\omega$  and  $k$  for further readability. We disregard the solution  $\omega_{\text{null}} = 0$  on the null space. On the column space, Eq. 11 reduces to

$$\omega^3 + i\omega^2 - \omega k^2 - ik^2(1 - \epsilon) = 0, \quad (12)$$

which can alternatively be written under the convenient form.

$$\omega^2 - k^2 + \frac{i}{\omega} (\omega^2 - k^2(1 - \epsilon)) = 0. \quad (13)$$

The change of variable  $\omega = iy$  gives a cubic with real positive coefficients

$$y^3 + y^2 + yk^2 + k^2(1 - \epsilon) = 0. \quad (14)$$

When Eq. 14 admits two complex conjugated roots and one real root, the latter is negative since  $k^2(1 - \epsilon) > 0$ . When Eq. 14 admits three real roots, Descartes' rule of sign shows that they are all negative. Since  $\Im(\omega) = \Re(y)$ , all modes of the DUSTYWAVE problem are damped. This result can alternatively be found from the argument principle (Debras et al. 2020). Let split  $\omega$  in its real and imaginary part by setting  $\omega \equiv r + is$ . One obtains

$$0 = r [r^2 - (3s^2 + 2s + k^2)], \quad (15)$$

$$0 = s^3 + s^2 + s(k^2 - 3r^2) + (k^2(1 - \epsilon) - r^2). \quad (16)$$

Eq. 15 shows that the three expected modes decompose as follow:

$$r = 0, \quad (17)$$

$$0 = s^3 + s^2 + sk^2 + k^2(1 - \epsilon), \quad (18)$$

and

$$r^2 = 3s^2 + 2s + k^2, \quad (19)$$

$$0 = s^3 + s^2 + s \frac{1}{4} (k^2 + 1) + k^2 \frac{\epsilon}{8}. \quad (20)$$

We note that the symmetry  $r \rightarrow -r$  implies three solutions  $\omega_{\pm} = \pm|r| + is$  and  $\omega_0 = is$ . Eqs. 17 – 18 give solutions that are always purely damped. Eqs. 19 – 20 give solutions that are contra-propagative and damped.

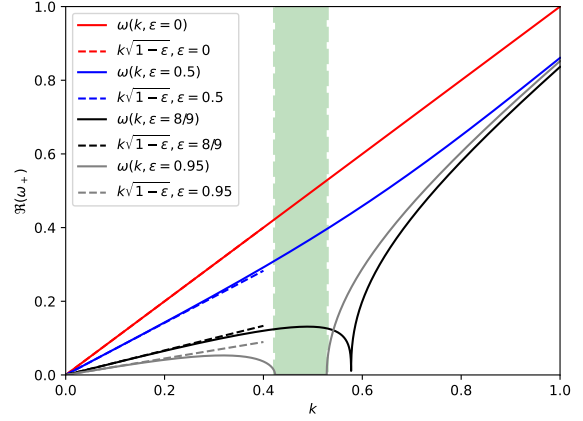


**Figure 2.** Real part of the root  $\omega_+$  for different values of the dust fraction  $\epsilon$  (solid lines) superimposed to the asymptotic regimes (dashed lines). A forbidden band develops for  $\epsilon \geq \epsilon_c = 8/9$ .

### 3 ABSENCE OF SOUND PROPAGATION

#### 3.1 Analysis

Fig. 2 shows that sound waves behave in a specific manner at large dust fractions. Above a critical value  $\epsilon_c$ , an interval of values for  $k$  where waves can not propagate develops (a so-called forbidden band). We relate the existence of the bifurcation at  $\epsilon_c$  to the fact that above this value, all three solutions come solely from Eq. 18. From the discriminant of the cubic Eq. 12, one gets the condition  $\epsilon \geq \epsilon_c = 8/9$  and  $k_{\text{min}} \leq k \leq k_{\text{max}}$  with

$$\begin{cases} k_{\text{min}} & \equiv \sqrt{\left(1 - \frac{9\epsilon}{8}\right) \left(3\epsilon - \frac{4}{3} + \sqrt{\epsilon\sqrt{9\epsilon - 8}}\right) + \frac{1}{3}}, \\ k_{\text{max}} & \equiv \sqrt{\left(1 - \frac{9\epsilon}{8}\right) \left(3\epsilon - \frac{4}{3} - \sqrt{\epsilon\sqrt{9\epsilon - 8}}\right) + \frac{1}{3}}, \end{cases} \quad (21)$$

The centre of the band  $k_c$  can be estimated from the relation

$$k_c^2 \equiv \sqrt{k_{\text{min}}^2 k_{\text{max}}^2} = \sqrt{1 - \epsilon}, \quad (22)$$

which indicates that the band is centred around  $k_c \sim (1 - \epsilon_c)^{1/4} = 1/\sqrt{3} \sim 0.57$ , except for values of  $\epsilon$  extremely close to unity (see Sect. 3.3 for the physical explanation). In that regime, this condition gives  $r^2 < 0$  in Eq. 18. This ensures three and only three complex roots for the dispersion relation as expected. Another quick way to find the critical value  $\epsilon_c = 8/9$  consists of solving for  $k$  as function of  $s$  in Eq. 18 to get  $k(s)^2 = \frac{-2s + 8s^2 + 8s^3}{2s + \epsilon}$ , which gives by enforcing  $r^2 < 0$  in Eq. 18,  $-2s^2 + (3\epsilon - 4)s - (1 - \epsilon) > 0$ . Positivity is ensured for positive discriminant, i.e.

$$\Delta = \epsilon(-8 + 9\epsilon) \geq 0 \Rightarrow \epsilon \geq \frac{8}{9}. \quad (23)$$

At the critical value  $\epsilon = \epsilon_c$ ,  $k = 1/\sqrt{3}$  and the dispersion relation Eq. 12 factorises according to  $(\omega + i/3)^3 = 0$ . Real and imaginary parts of  $e^{i\omega t}$  for the different modes at  $\epsilon = 0.95 > \epsilon_c$  are shown on Fig. 3. As expected, at  $k = 0.5$ , no mode propagates. This plot can be compared to the case  $\epsilon = 0.1$ , where the modes  $\omega_{\pm}$  propagate for any value of  $k$  (Fig. C1, Appendix C).

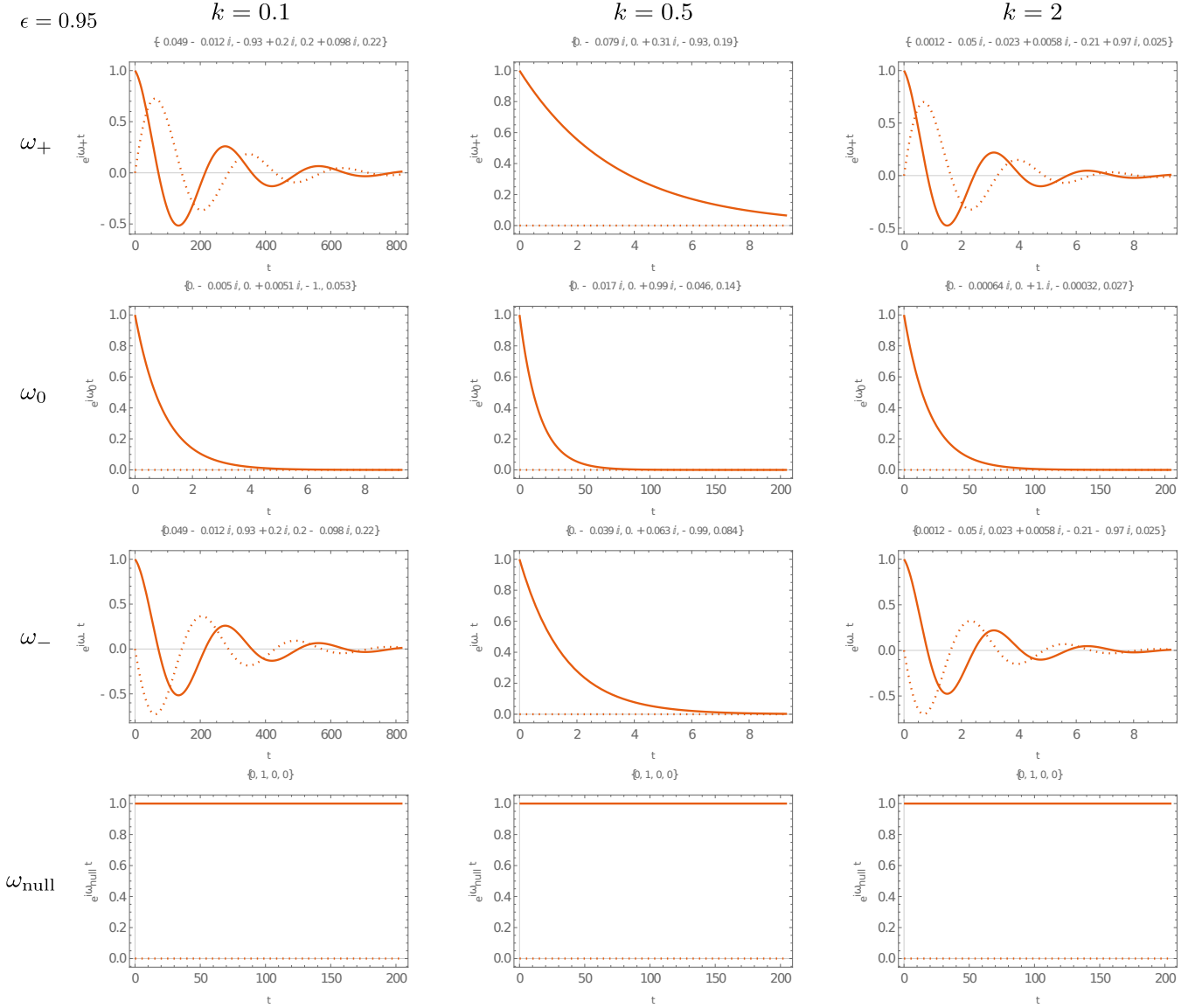


**Figure 3.** Real (solid line) and imaginary (dotted line) parts of  $e^{i\omega t}$  for the modes  $\omega_+$ ,  $\omega_0$  and  $\omega_-$  ( $\epsilon = 0.95$ ). The middle case  $k = 0.5$  corresponds to the regime where no mode propagates. Note the different timescales used for the plot for readability. The coefficients of the eigenvectors corresponding to the eigenvalues are provided on top of the plots and can be found in Table. B1–B2. The mode  $\omega_{\text{null}}$  corresponding to the null space of Eqs. 5–8 is provided for sanity check.

### 3.2 Eigenvectors

Fig. 4 shows the modulus (top) and the argument (bottom) of the eigenvectors corresponding to the modes  $\omega_+$ ,  $\omega_0$ ,  $\omega_-$  and  $\omega_{\text{null}}$  for values of  $k$  centred around the bifurcation. The amplitudes of the modes  $\omega_+$  and  $\omega_-$  are similar inside the forbidden band, although they are distinct outside. Differential phases of the mode  $\omega_0$  do not depend on  $k$ , outside or inside the band. Differential phases of the modes  $\omega_{\pm}$  are also constant inside the band. This ensures the required differential velocity from which the modes are damped. The mode  $\omega_{\text{null}}$  corresponds to a steady static perturbation on the dust density only, i.e.  $\delta\rho_g = 0$ ,  $\delta v_g = \delta v_d = 0$ .

### 3.3 Physical interpretation

In the limit  $\epsilon \rightarrow 0$ , the dispersion relation Eq. 12 reduces to

$$\omega^2 + i\omega - k^2 = 0. \quad (24)$$

Eq. 24 admits the solutions  $\tilde{\omega} = -i/2 \pm \sqrt{k^2 - 1/4}$ , showing the existence of  $k_{\text{max}} = 1/2$  below which waves are damped (in this limit,  $k_{\text{min}} = 0$ ). Physically, Eq. 24 is also the dispersion relation associated to the reduced system

$$\partial_t \delta\rho_g = -\rho_{g,0} \partial_x \delta v_g, \quad (25)$$

$$\partial_t \delta v_g = -\frac{K}{\rho_{g,0}} \delta v_g - c_s^2 \frac{\partial_x \delta\rho_g}{\rho_{g,0}}, \quad (26)$$

where the gas dissipates its energy in a passive dust phase through back-reaction. When  $(1 - \epsilon)$  is small but finite, large values of  $k^2/\omega$  can satisfy the dispersion relation, which reduces to  $i\omega^2 - \omega k^2 - ik^2(1 - \epsilon) = 0$ . This corresponds to propagation through

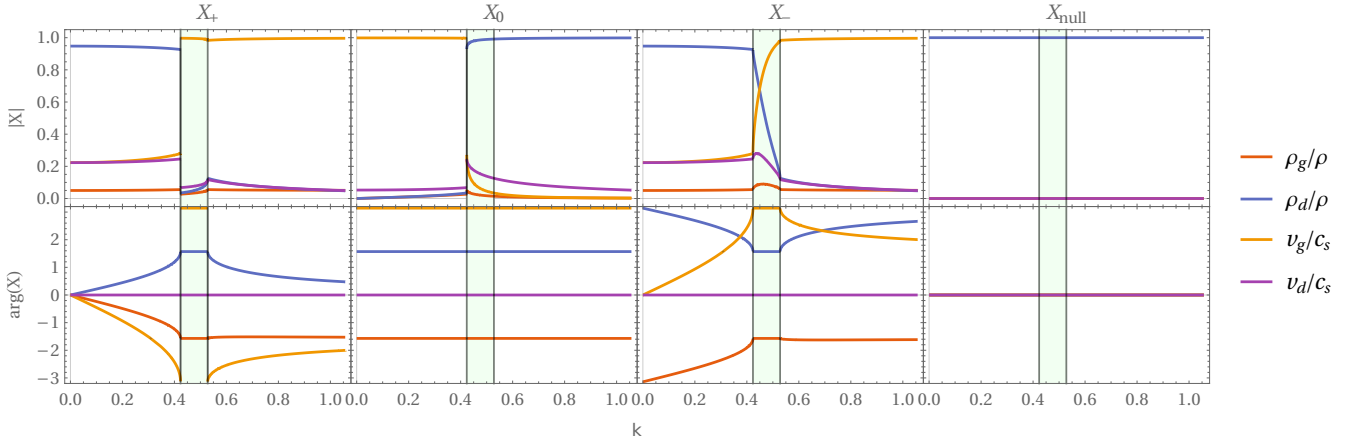


**Figure 4.** Modulus (top) and phase (bottom) of the eigenvectors at the **bifurcation** for the modes  $\omega_+$ ,  $\omega_0$  and  $\omega_-$  and  $\omega_{\text{null}}$  (from left to right,  $\epsilon = 0.95$ ). Values of the related eigen system can be found in Tables. B1 – B2.

the mixture and explains the finite value of  $k_{\text{min}}$  (e.g. Laibe & Price 2014b and App. A).

For the DUSTYWAVE problem with multiple dust species, the regime identified in this study exists when the stopping times of the different species are close enough (we verified this fact numerically). When this condition is not fulfilled, gas/mixture mode can propagate through one specie even if it can not through the other one, and no forbidden band is expected. This example provides a further situation where a physical effect observed in a mixture with a single grain size does not occur when several sizes are considered (e.g. Krapp et al. 2019).

## 4 CONCLUSION

We identified and characterised the existence of a regime in the single specie DUSTYWAVE problem where waves can not propagate, neither as a gas mode or a mixture mode. This regime develops above  $\epsilon_c = 8/9$ , when the dust-to-gas ratio is sufficiently large for gas to dissipate its energy in an independent dust phase via back-reaction. Numerical solvers can be checked in this regime to verify their accuracy at large dust fractions.

## ACKNOWLEDGEMENTS

GL acknowledges funding from the ERC CoG project PODCAST No 864965. This project has received funding from the European Union’s Horizon 2020 research and innovation programme under the Marie Skłodowska-Curie grant agreement No 823823. This project was partly supported by the IDEXLyon project (contract nANR-16-IDEX-0005) under the auspices University of Lyon. We acknowledge financial support from the national programs (PNP, PNPS, PCMI) of CNRS/INSU, CEA, and CNES, France. We used MATHEMATICA (Wolfram Research 14). We thank the anonymous referee for a thorough and insightful report and for suggesting the title.

## DATA AVAILABILITY

All relevant data are given in the article.

## APPENDIX A: ASYMPTOTIC BEHAVIOURS

When  $k \gg 1$  (the physical wavelength  $\lambda \equiv 2\pi c_s t_s/k$  is smaller than the physical stopping length  $c_s t_s$ ), Eqs. 17 – 20 provide

$$\begin{cases} \omega_+ &= \left[ +\sqrt{k^2 + 3\epsilon^2/4 - \epsilon} + \mathcal{O}(k^{-2}) \right] - i \left[ \epsilon/2 + \mathcal{O}(k^{-2}) \right], \\ \omega_0 &= -i \left[ (1 - \epsilon) + \mathcal{O}(k^{-2}) \right], \\ \omega_- &= \left[ -\sqrt{k^2 + 3\epsilon^2/4 - \epsilon} + \mathcal{O}(k^{-2}) \right] - i \left[ \epsilon/2 + \mathcal{O}(k^{-2}) \right], \end{cases} \quad (\text{A1})$$

or in a even more simplified form,

$$\begin{cases} \omega_+ &= [+k + \mathcal{O}(1)] - i \left[ \epsilon/2 + \mathcal{O}(k^{-2}) \right], \\ \omega_0 &= -i \left[ (1 - \epsilon) + \mathcal{O}(k^{-2}) \right], \\ \omega_- &= [-k + \mathcal{O}(1)] - i \left[ \epsilon/2 + \mathcal{O}(k^{-2}) \right]. \end{cases} \quad (\text{A2})$$

The evolution of the plane wave is correctly described by expanding both the real and the imaginary parts of  $\omega$  to their respective leading orders. In this gas regime, the propagation is supported by the pressure of the gas and damped by dust back-reaction. Since  $\Re(\omega_{\pm}) = \pm k + \mathcal{O}(1)$ , the typical physical oscillation time is  $\sim \lambda/c_s \ll t_s$ . After a typical time  $\sim (1 - \epsilon)^{-1} t_s$ , the initial dust velocity adjusts onto the one of the gas (mode  $\omega_0$ ). Meanwhile, the gas undergoes several oscillations that are supported by its own pressure (terms  $\pm k$ , modes  $\omega_{\pm}$ ) that are progressively damped by dust back-reaction (terms  $-i\epsilon/2$ , the factor 2 accounting for dissipation by both modes). In the limit  $k \ll 1$ , corresponding to  $\lambda \gg c_s t_s$ , one obtains

$$\begin{cases} \omega_+ &= +\sqrt{1 - \epsilon}k - i\epsilon k^2/2 + \mathcal{O}(k^3), \\ \omega_0 &= +i(-1 + \epsilon k^2) + \mathcal{O}(k^3), \\ \omega_- &= -\sqrt{1 - \epsilon}k - i\epsilon k^2/2 + \mathcal{O}(k^3). \end{cases} \quad (\text{A3})$$

In this mixture regime, the propagation is supported by both gas and dust simultaneously, and damped by an effective diffusion. The typical oscillation time for a perturbation satisfies  $\lambda/c_s \gg t_s$ . After a typical time  $t_s$ , the gas and dust velocities have relaxed towards the barycentric velocity of the mixture (mode  $\omega_0$ , factor  $-i$ ). Since the stopping time is much shorter than the oscillation time, the drag maintains the two phases well-coupled and the system tends to oscillate at the sound speed of the mixture  $c_s \sqrt{1 - \epsilon}$ , which accounts for the inertia of the dust (Laibe & Price 2012). Damping comes

from the  $-i\epsilon k^2/2$  term, which originates from the effective diffusion of the terminal velocity approximation (Laibe & Price 2014b).

## APPENDIX B: PARAMETERS FOR NUMERICAL TESTS

We provide parameters for numerical test – before ( $k = 0.1$ ), at ( $k = 0.5$ ) and after ( $k = 2.$ ) the bifurcation at  $\epsilon = 0.95$ . The eigenvalues  $\omega_+$ ,  $\omega_0$  and  $\omega_-$  are given in Table. B1. The corresponding values for the eigenvectors are given in Table. B2 Evolution of the densities and velocities are shown on Fig. 3.

## APPENDIX C: EVOLUTION AT LOW $\epsilon$

Evolution of the perturbations are given for  $\epsilon = 0.10 < \epsilon_c$ , for a purpose of comparison with Fig. 3. The regime where no mode propagates is not observed as expected.

## REFERENCES

- Ahuja A. S., 1973, *Journal of Applied Physics*, **44**, 4863  
 Baines M. J., Williams I. P., Asebiomo A. S., 1965, *MNRAS*, **130**, 63  
 Benítez-Llambay P., Krapp L., Pessah M. E., 2019, *ApJS*, **241**, 25  
 Booth R. A., Sijacki D., Clarke C. J., 2015, *MNRAS*, **452**, 3932  
 Clair B. P. L., Hamielec A. E., Pruppacher H. R., 1970, *Journal of the Atmospheric Sciences*, **27**, 308  
 Debras F., Mayne N., Baraffé I., Jaupart E., Mourier P., Laibe G., Goffrey T., Thuburn J., 2020, *A&A*, **633**, A2  
 Garaud P., Barrière-Fouchet L., Lin D. N. C., 2004, *ApJ*, **603**, 292  
 Gumerov N. A., Ivandaev A. I., Nigmatulin R. I., 1988, *Journal of Fluid Mechanics*, **193**, 53  
 Hubber D. A., Rosotti G. P., Booth R. A., 2018, *MNRAS*, **473**, 1603  
 Krapp L., Benítez-Llambay P., Gressel O., Pessah M. E., 2019, *ApJ*, **878**, L30  
 Laibe G., Price D. J., 2011, *MNRAS*, **418**, 1491  
 Laibe G., Price D. J., 2012, *MNRAS*, **420**, 2345  
 Laibe G., Price D. J., 2014a, *MNRAS*, **440**, 2147  
 Laibe G., Price D. J., 2014b, *MNRAS*, **440**, 2147  
 Laibe G., Price D. J., 2016, DUSTYWAVE: Linear waves in gas and dust (ascl:1602.004)  
 Lebreuilly U., Commerçon B., Laibe G., 2019, *A&A*, **626**, A96  
 Lorén-Aguilar P., Bate M. R., 2014, *MNRAS*, **443**, 927  
 Marble F. E., 1970, *Annual Review of Fluid Mechanics*, **2**, 397  
 McKinnon R., Vogelsberger M., Torrey P., Marinacci F., Kannan R., 2018, *MNRAS*, **478**, 2851  
 Mentiplay D., Price D. J., Pinte C., Laibe G., 2020, *MNRAS*, **499**, 3806  
 Moseley E. R., Squire J., Hopkins P. F., 2019, *MNRAS*, **489**, 325  
 Porth O., Xia C., Hendrix T., Moschou S. P., Keppens R., 2014, *ApJS*, **214**, 4  
 Price D. J., Laibe G., 2015, *MNRAS*, **451**, 813  
 Riols A., Lesur G., 2018, *A&A*, **617**, A117  
 Saffman P. G., 1962, *Journal of Fluid Mechanics*, **13**, 120  
 Stoyanovskaya O. P., Glushko T. A., Snytnikov N. V., Snytnikov V. N., 2018, *Astronomy and Computing*, **25**, 25  
 Stoyanovskaya O. P., Okladnikov F. A., Vorobyov E. I., Pavlyuchenkov Y. N., Akimkin V. V., 2020, *Astronomy Reports*, **64**, 107  
 Wolfram Research I., 14, Mathematica, Version 14.0, <https://www.wolfram.com/mathematica>  
 Yang C.-C., Johansen A., 2016, *ApJS*, **224**, 39

6 *David–Cléris & Laibe*

$\omega$	$k = 0.1$	$k = 0.5$	$k = 2.$
$\omega_+$	$0.0219514 - 0.00479354i$	$-0.639778i$	$1.93044 - 0.474696i$
$\omega_0$	$-0.990413i$	$-0.0665243i$	$-0.0506079i$
$\omega_-$	$-0.0219514 - 0.00479354i$	$-0.293697i$	$-1.93044 - 0.474696i$

**Table B1.** Eigenvalues for numerical tests of the DUSTYWAVE regime ( $\epsilon = 0.95$ ).

${}^\top X = \left( \frac{\delta \rho_g}{\rho_0}, \frac{\delta \rho_d}{\rho_0}, \frac{\delta v_g}{c_s}, \frac{\delta v_d}{c_s} \right)$	$k = 0.1$	$k = 0.5$	$k = 2.$
$X_+$	$\begin{pmatrix} 0.0117633 + 0.0486907i \\ -0.20202 + 0.925123i \\ 0.098324 + 0.202488i \\ 0.223959i \end{pmatrix}$	$\begin{pmatrix} 0.0388307 \\ -0.0625475 \\ -0.993722i \\ 0.0842453i \end{pmatrix}$	$\begin{pmatrix} 0.0501937 + 0.00123333i \\ -0.00576226 + 0.0234334i \\ 0.974816 - 0.214459i \\ 0.0252485i \end{pmatrix}$
$X_0$	$\begin{pmatrix} 0.00504115 \\ -0.00509254 \\ -0.998564i \\ +0.0530918i \end{pmatrix}$	$\begin{pmatrix} 0.0172053 \\ -0.98915 \\ -0.0457829i \\ +0.138532i \end{pmatrix}$	$\begin{pmatrix} 0.000639653 \\ -0.999645 \\ -0.000323715i \\ +0.0266263i \end{pmatrix}$
$X_-$	$\begin{pmatrix} 0.0117633 - 0.0486907i \\ -0.20202 - 0.925123i \\ -0.098324 + 0.202488i \\ +0.223959i \end{pmatrix}$	$\begin{pmatrix} 0.0790522 \\ -0.308168 \\ -0.928696i \\ +0.190543i \end{pmatrix}$	$\begin{pmatrix} 0.0501937 - 0.00123333i \\ -0.00576226 - 0.0234334i \\ -0.974816 - 0.214459i \\ +0.0252485i \end{pmatrix}$
$X_{\text{null}}$	$\begin{pmatrix} 0 \\ i \\ 0 \\ 0 \end{pmatrix}$	$\begin{pmatrix} 0 \\ i \\ 0 \\ 0 \end{pmatrix}$	$\begin{pmatrix} 0 \\ i \\ 0 \\ 0 \end{pmatrix}$

**Table B2.** Eigenvectors for numerical tests of the DUSTYWAVE regime ( $\epsilon = 0.95$ ).

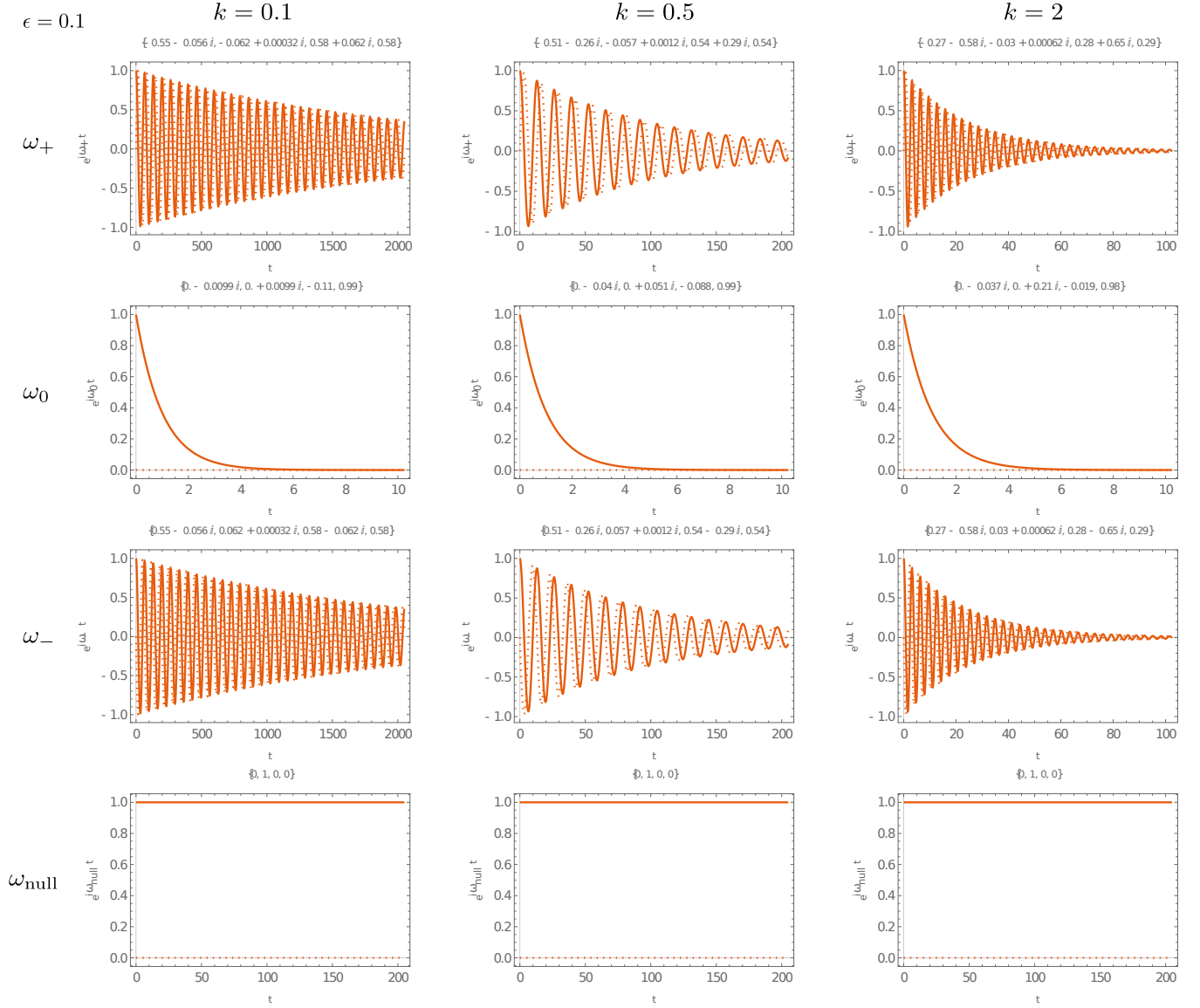


**Figure C1.** Real (solid line) and imaginary (dotted line) parts of  $e^{i\omega t}$  for the modes  $\omega_+$ ,  $\omega_0$  and  $\omega_-$  and  $\omega_{null}$  ( $\epsilon = 0.10$ ). No regime is observed in this case and at least 2 modes propagate through the mixture.